Asian Journal of Physics
Vol. 31, No 1 (2022)1-16
Available on: www.asianjournalofphysics.in

ap

On the methods to determine the focal length of an imaging system: A tutorial approach

Rajpal S Sirohi

Alabama A&M University Normal, Alabama, USA

This article is dedicated to late Prof B N Gupta

Focal length of an imaging system is an important parameter as it determines its gathering power, numerical aperture and resolution. Its determination becomes very difficult as one of the planes is not physically accessible. A number of methods have been developed that measure either the effective focal length or the back focal length. The objective of the present paper is to discuss various methods that have been investigated and reported in the literature.

Keywords: Focal length, Radius of curvature, Nodal slide, Interferometry.

1 Introduction

Focal length of an imaging system is a very important parameter as it controls the magnification, gathering power, resolution directly or indirectly. The focal length is the distance between the focal plane and corresponding principal plane. Focal plane is a physical plane and is accessible for measurement. Principal plane is a mathematical plane and is not accessible physically. Therefore, the determination of focal length poses problems. Further, the procedure tends to be more complex if the magnitude of focal length is either very small (~mm) or very large (~several meters). If focal length is to be measured with high accuracy, the measurement procedure tends to be more complex and expensive.

The paper describes several methods of focal length measurement and also makes comments on the accuracy of measurement.

2 What is a focal length?

Consider a thick bi-convex lens of central thickness d and bounded by two spherical surfaces of radii of curvature of R_1 and R_2 as shown in Fig 1.

The convex lens is characterized by six planes - two focal planes, two principal planes and two nodal planes. Their intersections with the optical axis are two focal points, two principal points and two nodal points represented by F, F', H, H', N and N', respectively. The distances are measured from the vertices *V* and *V'*. The distance between *H* and *F* is the front effective focal length *f* and the distance between *H'* and *F'*, is the back effective focal length. The distance between V and V'. is the thickness or axial distance *d* of the lens. The distances measured along the direction of ray propagation are taken positive and those opposite are taken as negative. Actual rays are shown with solid lines. The principal planes are planes of unit lateral magnification and nodal planes are planes of unit angular magnification. Principal planes and nodal planes are mathematical description. Various distances as marked in the Fig 1 are given below:

Corresponding author
e mail: rs_sirohi@yahoo.co.in (Rajpal S Sirohi)

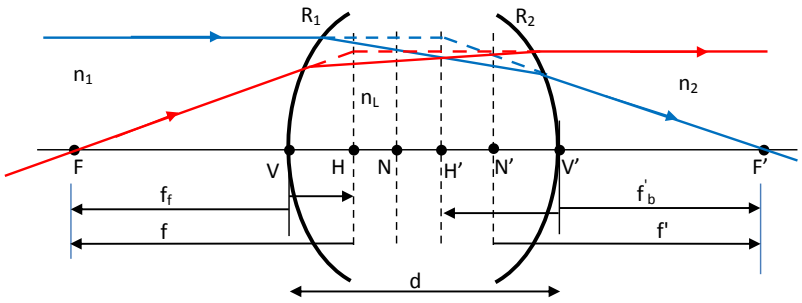

Fig 1. A thick bi-convex lens: refractive index in object space is n_1 and in image space is n_2

Various distances as marked in the Fig 1 are given below:

$$\mathrm{VF} = -f'\left(1-\frac{d}{f_2'}\right) \qquad \mathrm{VH} = f\frac{d}{f_2'}$$

$$\mathrm{V'F'} = f'\left(1-\frac{d}{f_1'}\right) \qquad \mathrm{V'H'} = -f'\frac{d}{f_1'}$$

$$\mathrm{HN} = f'\frac{n_2-n_1}{n_2} \qquad \mathrm{H'N'} = f\frac{n_1-n_2}{n_1}$$

where

$$-\frac{n_1}{f_1}=\frac{n_L}{f_1'}=\frac{n_L-n_1}{R_1} \qquad \frac{n_L}{f_2}=-\frac{n_2}{f_2'}=\frac{n_2-n_L}{R_2}$$

The front and back effective focal lengths are given by

$$-\frac{n_1}{f}=\frac{n_2}{f'}=\frac{n_L}{f_1'}+\frac{n_2}{f_2'}-\frac{d\,n_L\,n_2}{f_1'\,f_2'}$$

Here f_1 and f_1' are the front and rear focal lengths of the first refracting surface of radius of curvature R_1 and f_2 and f_2' of the second refracting surface of radius of curvature R_2.

This is a general case. A lens can have many focal lengths depending on the refractive index of the medium in which it is immersed or the medium in the image space. In most of the applications, the media in front and back of the lens are the same, i.e., $n_1 = n_2$. In this case, the principal planes coincide with the nodal planes and the front and back focal length are equal in magnitude. Further, when the optical system suffers from aberrations, it can be assigned multiple focal lengths. In what follows, the optical systems are assumed to be diffraction limited. .

3 Methods to measure the focal length

It may be remarked that not all the methods measure the effective focal length. Some methods measure the back focal length, some effective focal length and some radius of curvature of the wave exiting from the optical system. The methods are grouped under the following sub-headings:

3.1 Auto-collimation method

3.2 y'/tan θ method or Porr's method

3.3 Focimeter

3.4 Nodal Slide method

3.5 Imaging conjugates method

3.6 Cornu method

3.1 Auto-collimation method

An image of the object is formed on itself in this method as shown in the Fig 2. The object could be a point source (pin-hole) or an extended object like a mesh or a grating.

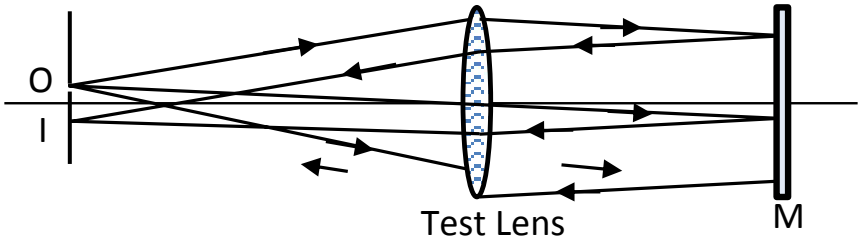

Fig 2. A schematic of an auto-collimation method.

In the Fig 2, O is a pin-hole which is placed slightly off-axis so that its image does not fall on itself but is slightly displaced. Mirror M retroreflect the beam from the lens under test. The lens is moved on the optical axis until a sharp image I is formed on the object plane. The distance between the vertex of the test lens and the image plane can be measured with a distance measuring interferometer. The method measures the back focal length. The accuracy depends on the accuracy of the distance measuring device and the accuracy with which the image plane is located.

Another convenient way is to use a single mode fiber for illumination as well as for receiving the retroreflected beam. The lens is displaced until the light coupled to the single mode fiber is maximized. This happens when the tip of the fiber is at the focal point of the test lens.

3.2 y'/tanθ method

The method uses a collimator with a reticle placed at its focal plane. The reticle may be a pair of parallel lines with their spacing y_c precisely known. It is illuminated by an incoherent source. The image of the reticle is formed at infinity. The test lens whose focal length f' is to be measured, makes the image of the reticle at its focal plane and the spacing y' of the lines in the image is measured with a travelling microscope.

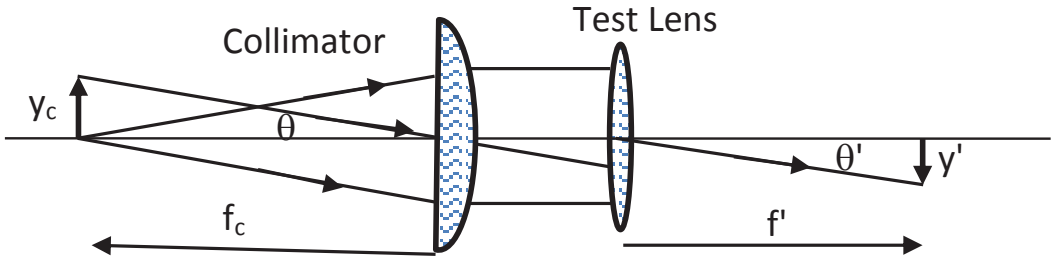

Fig 3. A schematic of *y'/tanθ* method to measure the focal length of a positive lens.

From Fig 3, we have

$$\frac{y_c}{f_c} = \frac{y'}{f'} \rightarrow\rightarrow\rightarrow f' = f_c \frac{y'}{y_c}$$

The focal length f_c of the collimator is precisely known. Therefore, the focal length of the test lens can be measured relatively easily.

The focometer is an adaptation of $y'/\tan\theta$ method, in which the image height y' is related to the focal length as

$$y' = -f \tan\theta = f' \tan\theta'$$

where θ is the angle subtended by an object at infinity. Since the media on both sides of the lens are the same, the nodal planes coincide with the principal planes and hence $\theta = \theta'$. The uncertainty in focal length measurements is obtained from

$$u_{f'} = \sqrt{\left(\frac{\partial f'}{\partial y'}\right)^2 u_{y'}^2 + \left(\frac{\partial f'}{\partial \theta}\right)^2 u_\theta^2} = f' \sqrt{\left(\frac{u_{y'}}{y'}\right)^2 + \left(\frac{2u_\theta}{\sin 2\theta}\right)^2} = f' \sqrt{\left(\frac{u_{y'}}{y'}\right)^2 + \left(\frac{u_\theta}{\theta}\right)^2}$$

where $u_{y'}$ and u_θ are the uncertainties in the measurement of y' and angle θ, respectively. This method sometimes is called the Porr's method.

3.3 Using a Focimeter

A focimeter consists of a collimator with a reticle placed at its focal plane. The image of the reticle is formed at infinity. A focusing lens brings this image from infinity to its focal plane as shown in Fig 4.

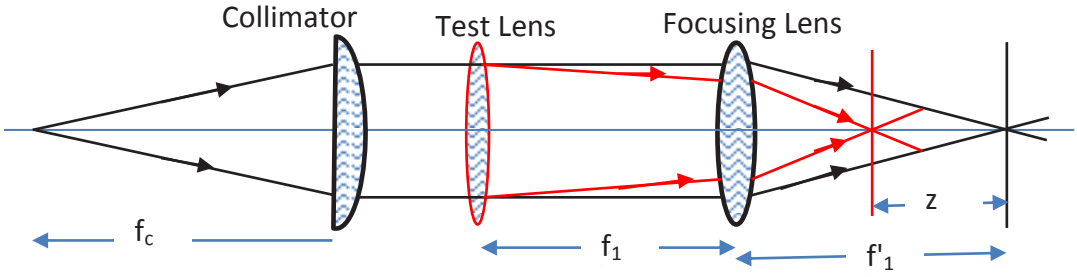

Fig 4. Working principle of a focimeter.

When a test lens is placed at the front focal plane of the focusing lens, the image plane shifts inwards if the test lens is positive. The distance z is the shift of the image plane, which is measured. The focal length f' of the test lens is obtained from the expression

$$f' = \frac{f_1'^2}{z}$$

This expression is valid when both the lenses are considered thin. The role of the collimator is to provide a collimated beam. The focal length of the focusing lens should be accurately known. The method can be used to measure focal length of both the positive and negative lenses. The range of focal lengths that can be measured is determined by the focal length of the focusing lens.

The uncertainty $u_{f'}$ in the measurement of focal length f' is obtained from

$$u_{f'} = f' \sqrt{\left(\frac{2}{f_1}\right)^2 u_{f_1}^2 + \left(\frac{1}{z}\right)^2 u_z^2}$$

In practice, the lenses have a finite thickness and the focusing lens may be a highly corrected lens system. It is, therefore, appropriate to consider the lenses with their cardinal points. Figure 5 shows a schematic of a lens combination that is placed in a collimated beam.

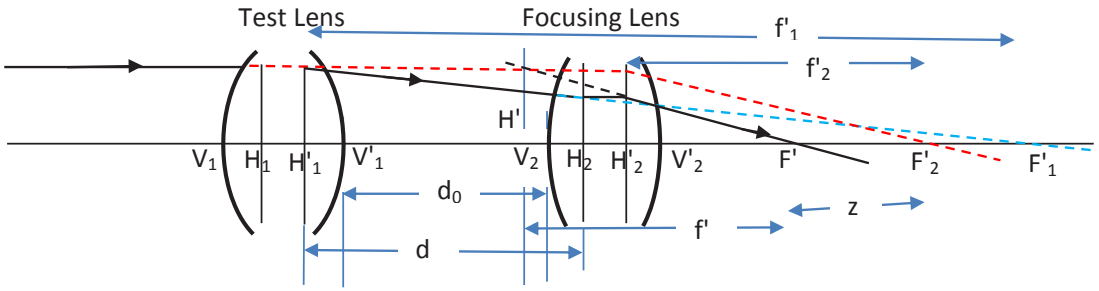

Fig 5. Various notations used for thick lens combination.

Initially without test lens in the collimated beam, the beam is focused at F_2', which is the focal point of the focusing lens. When test lens is inserted in the beam, the focal point shifts by z inwards to F′, which is now the focal point of the lens combination. The focal length f_1' of the test lens is obtained from the expression

$$f_1' = d - f_2' + \frac{f_2'^2}{z}$$

The focal length is obtained by measuring d, z and f_2'. In fact, z is measured for several values of d. Under thin lens approximation and the condition $d = f_2$, it reduces to

$$f_1' = \frac{f_2'^2}{z}$$

3.4 Nodal Slide

The method is based on the following

i. If the object space and image space refractive indices are identical, the principal planes coincide with the nodal planes,

ii. A rotation about the nodal point does not rotate/shift the image.

A collimator with a reticle at its focal plane provides a collimated beam. Test lens is placed in the collimated beam on a nodal slide. It is adjusted such that the vertex V′ is on the axis of rotation. Figure 6 shows the schematic.

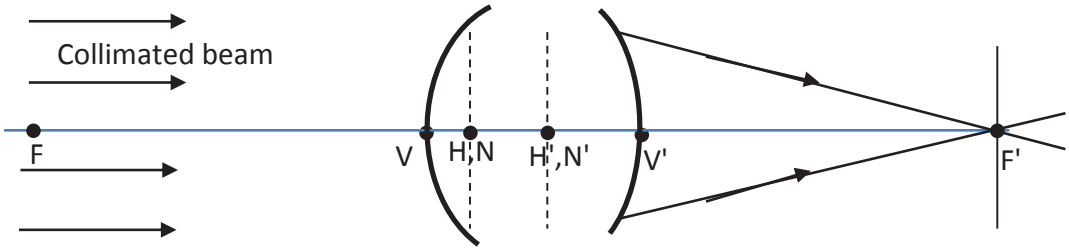

Fig 6. A schematic of nodal slide method.

Now the travelling microscope is focused on the vertex V′ and its position is noticed on the nodal slide scale. The travelling microscope is now translated to focus it on the image, which is formed at the focal plane passing through F′, and its position is noted. The difference between these two readings gives the back focal distance f_B'.

Keeping the microscope focused on the image, the nodal slide is translated such that the axis of rotation passes through the rear nodal point N'. In this case, a rotation of the lens will not displace the image. This position of the nodal slide is noted. The difference between these two positions is the distance N′ V′. This distance is added to the back focal distance to obtain the effective rear focal length f' of the lens.

The method involves the measurements of two distances namely V′F′ and N′V′ requiring that the traveling microscope is focused at two locations and ascertaining the position of axis of rotation. The distances can be measured quite accurately using a distance measuring interferometer. But the location determination is by the travelling microscope whose depth of focus plays a significant role in the overall uncertainty of the focal length measurement. The depth of focus depends on the numerical aperture, *NA*, of the microscope objective. It is given by $\Delta z_{dof} \sim \lambda/NA^2$: the numerical aperture *NA* is given by *NA* ~ 1/(2F#). Therefore, a short focal length lens has a smaller depth of focus. However, in many a situations longer focal length objective may be needed to access the point N′.

3.5 Measurement of imaging conjugates

3.5.1 Point object at several locations

Figure 7 shows an imaging geometry in which an object point O is imaged as an image point I. The imaging is governed by the paraxial imaging equation

$$\frac{1}{q} - \frac{1}{p} = \frac{1}{f'}$$

where the object distance *p* and image distance *q* are measured from the principal planes.

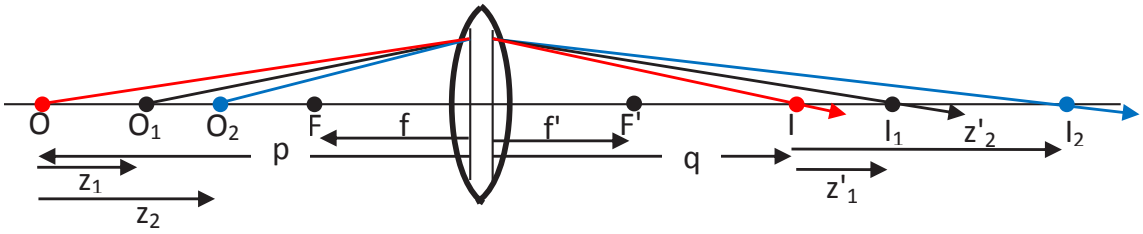

Fig 7. Imaging of point sources placed at different locations.

When the object O is translated to new location O_1, its image moves to the new position I_1.The distance z_1 and z_1' can be measured accurately. The object is again moved to another position O_2 and its image moves to the new location. The distance z_2 and z_2' are measured. Using the measured distances z_1, z_1', z_2 and z_2', the focal length of the lens is obtained from

$$f'^2 = \frac{\alpha z_2^2 + \beta z_1^2 - z_1\, z_2\, (\alpha + \beta)}{(\alpha - \beta)^2}$$

where α and β are: $\alpha = z_1/z_1'$ and $\beta = z_2/z_2'$. Positive root is taken as the focal length.

In a modification of this method, the point O is taken at infinity. The points O_1 and O_2 are at a distance p_1 and p_2 from the principal planes. The images of these points are at a distance q_1 and q_2 from the principal plane, respectively. The focal length is obtained from the formula

$$f' = \sqrt{\frac{KLM}{K-L}}$$

where $K = q_1 - q$; $L = q_2 - q$; $M = p_2 - p_1$. Here $q = f'$. The uncertainty $u_{f'}$ can be shown to be given by

$$u_{f'} = \frac{1}{2f'} \frac{1}{(L-K)^2} \sqrt{L^4 M^2 u_K^2 + K^4 M^2 u_L^2 + K^2 L^2 (L-K)^2 u_M^2}$$

where u_K, u_L and u_M are the uncertainties in the measurements of *K*, *L* and *M*, respectively.

In another modification, the point source O is translated in equal steps, i.e., $z_1 = z_2 = z$. It can be shown that the focal length f' is obtained as

$$f'^2 = 2z\, z_1' z_2' \frac{z_2' - z_1'}{(z_2' - 2z_1')^2}$$

3.5.2 Two conjugate positions

If the distance between the conjugate positions is greater than four times the focal length of the lens to be measured, then two positions of the lens can be found. The method involves the measurement of the distance between the conjugate positions and the distance between the positions of the lens. Let the distance between the conjugate positions be L and the distance between the two positions of the lens be d. The focal length is obtained from the expression

$$f' = \frac{L^2 - d^2}{4L}$$

It can be shown that the product of magnifications is unity. The uncertainty in focal length measurement is obtained from

$$u_{f'} = \sqrt{\left(\frac{L^2 + d^2}{4L^2}\right)^2 u_L^2 + \left(\frac{d^2}{4L^2}\right)^2 u_d^2}$$

where u_L and u_d are the uncertainties in the measurement of length L and length d, respectively.

3.5.3 Magnification method

Following the imaging equation, we write this in terms of the magnification as

$$\frac{1}{q} - \frac{1}{-p} = \frac{1}{f'} \rightarrow\rightarrow 1 - \frac{q}{-p} = \frac{q}{f'} = (1 - m) \rightarrow\rightarrow q = f'(1 - m);\ m = -\frac{q}{-p}$$

Now, the object is displaced by z that results in the shift of image plane by z'. The magnification m_1 is measured at this plane. Therefore, using the imaging equation we have

$$\frac{1}{q - z'} - \frac{1}{p + z} = \frac{1}{f'} \rightarrow\rightarrow 1 - \frac{q - z'}{p + z} = \frac{q - z'}{f'} = (1 - m_1) \rightarrow\rightarrow q = z' + f'(1 + m_1)$$

Substituting the value of q, we obtain

$$f'(1 - m) = z' + f'(1 - m_1) \rightarrow\rightarrow f' = \frac{z'}{m_1 - m}$$

The method involves measurement of one distance and two magnifications. The uncertainty in the focal length measurement is given by

$$u_{f'} = \sqrt{\left(\frac{f'}{z'}\right)^2 u_{z'}^2 + 2f'^2 \left(\frac{f'}{z'}\right)^2 u_m^2}$$

It has been assumed that the uncertainty in the measurement of m and m_1 is the same.

3.6 Cornu method

The test lens is illuminated with a collimated beam from a collimator with a reticle on its focal plane as shown in Fig 8. The image of the reticle is formed by the test lens at its rear focal plane. This image is seen by a travelling microscope and its position is noted. The microscope is translated towards the test lens and is focused on the rear vertex V′ and its position is noted. The difference between these two readings gives the distance V′F′, which is the rear back focal distance. Now the microscope is focused on V_I, which is the image of vertex V formed by the test lens. The difference between the first reading and this reading of the microscope gives the distance $V_I F'$.

Now the lens is flipped, and same procedure is repeated, thereby measuring the distance VF, which is the front focal distance, and the distance V_I'F, where V_I' is the image of V′ formed by the test lens.

The focal length is calculated from

$$f \times f' = f^2 = VF \times V_I F' = V' F' \times V_I' F$$

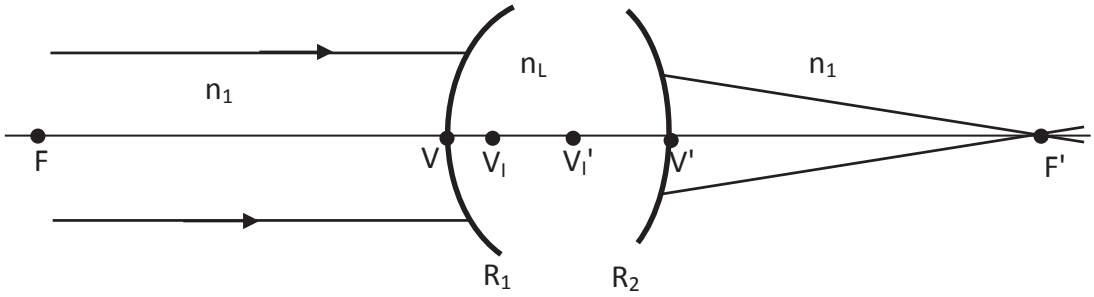

Fig 8. V_I is the image of V formed by the lens and V_I' is the image of V' formed by the lens.

The method involves essentially measurement of two distances which are obtained by focusing the travelling microscope at least at four places. Assuming that the depth of focus error is exceedingly small compared to the error in distance measurement, the uncertainty in the focal length measurement can be expressed as

$$u_{f'} = \frac{1}{2f'}\sqrt{d_2^2 + u_{d1}^2 + d_1^2 + u_{d2}^2} \cong \frac{u_d}{2f'}\sqrt{d_2^2 + d_1^2}$$

where we have used the relation $f = \sqrt{d_1 d_2}$ and taken the uncertainties in measurement of d_1 and d_2 as equal.

3.7 Moiré Deflectometry

The method is based on a fact that two gratings of slightly different pitches aligned with their element parallel produce a moiré fringe pattern due to the pitch mis-match. In order to use this fact, two identical gratings aligned with their elements parallel and separated by a distance are placed in the convergent beam as shown in Fig 9.

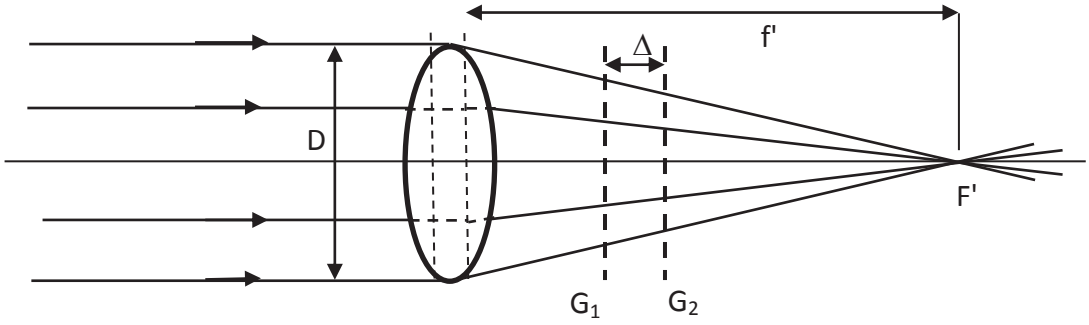

Fig 9. A schematic of moiré deflectometry – G_1 and G_2 are the linear gratings.

Let the pitch of the identical gratings G_1 and G_2 be p and the radius of the illuminated patch at grating G_1 be a and at grating G_2 be b. Therefore, the grating G_1 of size $2a$ is projected on the grating G_2 of size $2b$. The pitch p' of the projected grating G_1 is $p' = p\,b/a$. Due to pitch mis-match, a moiré fringe pattern is formed. The pitch d of the moiré fringe pattern is

$$d = \frac{pp'}{p - p'} = \frac{p\,\frac{b}{a}}{1 - \frac{b}{a}} = p\,\frac{b}{a - b}$$

Further from the figure,

$$\frac{D}{f'} = \frac{2(a-b)}{\Delta} \rightarrow\rightarrow f' = \frac{\Delta D d}{2p\,b} = \frac{\Delta D}{p\,n}$$

where n ($2b/d$) is the number of the moiré fringes formed on the grating G_2. In fact, one can count the number of fringes as a function of Δ by translating grating G_1 and obtain the focal length from the slope of the line. The method could be used to measure long focal lengths.

The uncertainty in the measurement of focal length is obtained as

$$u_f = f' \sqrt{\frac{1}{\Delta^2}u_\Delta^2 + \frac{1}{D^2}u_D^2 + \frac{1}{p^2}u_p^2 + \frac{1}{n^2}u_n^2}$$

where u_Δ, u_D, u_p and u_n are the uncertainties in the measurement of Δ, D, p and n, respectively.

In a modification of the technique, the gratings G_1 and G_2 with the grating elements vertical (y-axis) are slightly rotated by a small angle ($+\theta$ and $-\theta$) with the vertical resulting in the formation of a moiré fringe pattern with fringe running horizontally i.e., parallel to the x-axis. This is achieved in collimated illumination. When the test lens is inserted in the beam, the gratings are illuminated with a convergent beam. If the radius of curvature of the spherical wave is R at the grating G_1, then the moiré fringes make an angle ϕ with the axis. The radius of curvature R is then obtained from

$$R = \frac{\Delta}{\theta \tan\phi} + \Delta$$

Note that the method measures the radius of curvature and not the focal length. If the grating G_1 is in contact with the lens, then it measures the back focal length.

3.8 Talbot Interferometry

The method makes use of the Talbot phenomenon. A grating illuminated with a collimated beam reproduces itself at equi-spaced planes which are separated by the Talbot distance. It also self-images when illuminated by a diverging or converging wave but the Talbot planes are not equi-spaced and the pitch in the self-images is different than that of the grating.

The method uses a pair of identical gratings: second grating is placed at the Talbot plane of the first grating and the grating is rotated slightly in its own plane thereby producing moiré fringe pattern. Initially grating G_1 is illuminated by a collimated beam and grating G_2 is placed at its self-image plane. Assuming the grating elements of G_1 and G_2 to be vertical (y-axis) initially, the gratings are rotated by a small amount, $\pm\theta$, in its own plane: one grating is rotated clockwise and the other grating anti-clockwise. This forms a moiré fringe pattern in which moiré fringes are horizontal (x-axis). The pitch d of the moiré fringe is $d = p/2\sin\theta$, where p is the pitch of the grating G_1 or G_2. This is the initial setting. Now the test lens is introduced and is kept close to grating G_1 as shown in the Fig 10.

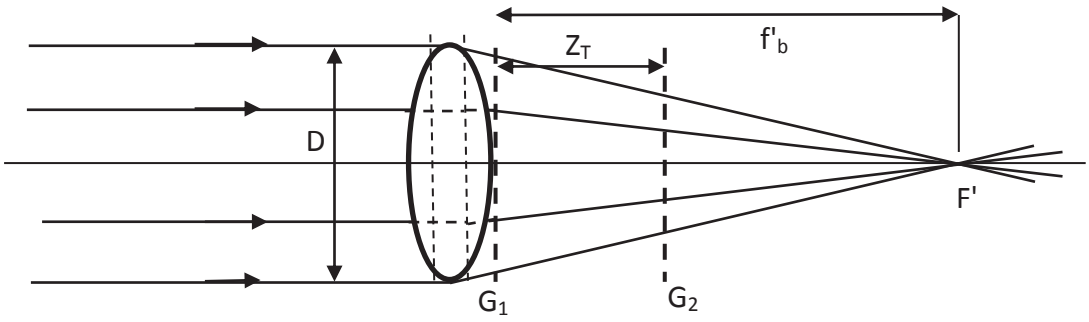

Fig 10. A schematic of Talbot interferometry – G_1 and G_2 are gratings, Z_T is Talbot distance.

The grating G_1 is illuminated by a wavefront that has a radius of curvature f_b' and hence its pitch will change. The pitch p' of grating G_1 at its n^{th} self-image plane is given by

$$p' = \frac{p\lambda f_b'}{\lambda f_b' + np^2}$$

Assuming the focal length to be sufficiently large such that the self-image plane distance does not change appreciably due to illumination by a convergent wave, the moiré fringe pattern is formed between the gratings of slightly different pitches resulting in the rotation of the moiré fringe pattern. The angle of rotation ϕ with the x-axis is given by

$$\tan\phi = \frac{p - p'}{p + p'}\cot\theta$$

and the pitch of the moiré fringes is given by

$$d = \frac{pp'}{p + p'}\frac{\cos\phi}{\sin\theta} = \frac{pp'}{(p^2 + p'^2 - 2pp'\cos 2\theta)^{1/2}}$$

The angle of rotation ϕ is measured, and the focal length is calculated from

$$f_b' = (\cot\theta\cot\phi - 1)\frac{np^2}{2\lambda}$$

The expression for focal length in above equation is different than the reported expression, which is obtained when one of the gratings G_1 is vertical and the other grating G_2 is inclined at an angle θ with the vertical.

The method measures the back focal length of the lens. It is a convenient method to measure long focal lengths.

The uncertainty in the measurement of back focal length can be obtained from the formula

$$u_{f_b'} = f_b'\sqrt{\left(\frac{1}{\cot\theta\cot\phi - 1}\right)^2\left[\left(\frac{\cot\phi}{\sin^2\theta}\right)^2 u_\theta^2 + \left(\frac{\cot\theta}{\sin^2\phi}\right)^2 u_\phi^2\right] + \frac{1}{n^2}u_n^2 + \frac{2}{p^2}u_p^2 + \frac{1}{\lambda^2}u_\lambda^2}$$

Talbot interferometry can also be used for focal length measurement in another way. It is essentially an extension of a method described under section 3.5.1. Figure 11 shows the schematic of the method. A grating G is placed in a collimated beam. Self-images of the grating which are equi-spaced are formed. The separation between the consecutives self-images is the Talbot distance Z_T. Test lens images these self-images according to the lens equation. The location of these images is found using another grating that forms the moiré pattern. It may be noted that the orientation and the pitch of moiré fringes will be different for different images due to pitch mismatch caused by lens magnification. In contrast to the method discussed in section 3.5.1, Talbot phenomenon provides equi-spaced objects positions for imaging by the test lens.

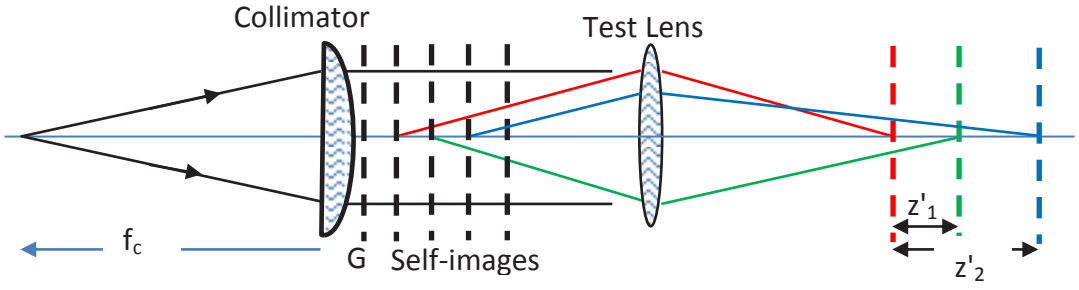

Fig 11. Self-images as objects for measuring focal length.

3.9 Fizeau Interferometry

A lens changes the curvature of incident wave and Fizeau interferometry converts this curvature of the wavefront into circular interference fringes. Figure 12 shows a schematic of a Fizeau interferometer. A collimator provides a collimated beam, a part of this beam is reflected by a reference surface R, which acts as a reference beam. This beam, on reflection from a beam splitter, falls on the screen. The collimated beam is brought to focus by the test lens. A mirror placed at the focal plane of the test lens will retro-reflect it. This beam, on reflection from the beam splitter falls on the screen where an interference pattern is observed. By manipulating the mirror, a fringe free field (uniform irradiance) is obtained. This is the null condition and arises due to interference between the two collimated beams propagating along the same direction. If the mirror is displaced by an amount d from this position, the reflected beam will appear arising from a point source which is $2d$ distant from the focal point and hence the wave exiting from the test lens will be a convergent wave. Superposition of a convergent wave and a collimated wave will produce a Newton's ring type fringe pattern.

It can be shown that when the point source is displaced away from the focal point by Δf, the radius of curvature R of wave after transmission through the lens of focal length f will be $f(f+\Delta f)/\Delta f$ and the wavefront will be converging. An expanded version of the beams near the mirror under two different conditions is shown as a sub-set. The amplitude $u(x, y)$ of the wavefront on the screen is expressed as

$$u(x, y) \propto e^{ik((x^2+y^2)/2R)} = e^{ik\frac{x^2+y^2}{f(f+2d)}d}$$

where d is the displacement of the mirror away from the focal plane. A collimated wave generated by the reference surface R and the convergent wave $u(x, y)$ interfere to produce circular fringes on the screen. The interference condition can be expressed as

$$\frac{x^2+y^2}{f(f+2d)}d = m\lambda$$

where m is the fringe order and λ is the wavelength. The radius r_m or the diameter D_m of the m^{th} fringe is expressed as

$$r_m^2 = m\lambda\frac{f(f+2d)}{d} \text{ or } D_m^2 = 4m\lambda\frac{f(f+2d)}{d}$$

From this, we obtain

$$f^2 + 2fd - \frac{D_{m+n}^2 - D_m^2}{4n\lambda}\cdot d = 0$$

From this the focal length is obtained as

$$f = -d + d\sqrt{1 + \frac{D_{m+n}^2 - D_m^2}{4n\lambda d}}$$

However, if the mirror is moved by d towards the lens, the focal length is obtained from

$$f = d + d\sqrt{1 + \frac{D_{l+m}^2 - D_l^2}{4n\lambda d}}$$

where D_l^2 is the diameter of the l^{th} ring formed in the second interference pattern. When both the interference patterns are utilized, the focal length can be expressed as

$$f = \frac{d}{2}\left[\sqrt{1 + \frac{D_{m+n}^2 - D_m^2}{4n\lambda d}} + \sqrt{1 + \frac{D_{l+m}^2 - D_l^2}{4n\lambda d}}\right]$$

If the focal length of a negative lens is to be determined, additional optical component of an appropriate and known curvature or focal length is needed. It can be either a mirror or a positive lens.

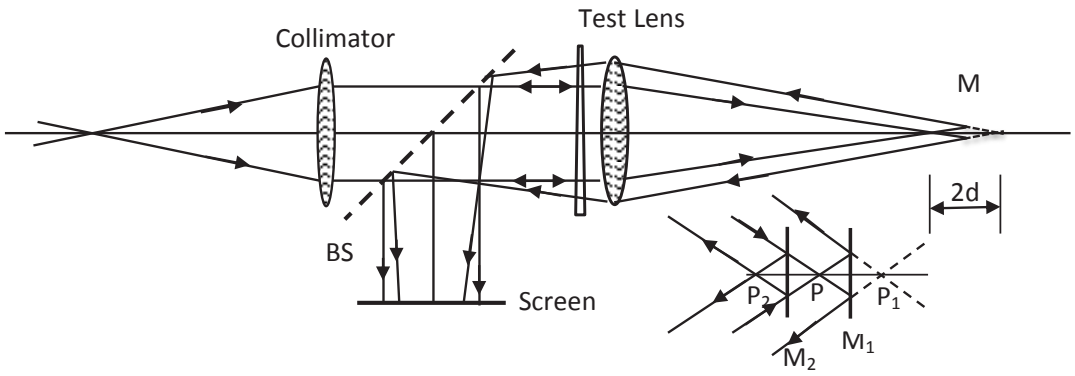

Fig 12. A Fizeau interferometer to determine the focal length of a positive lens.

3.10 Diffraction at a linear grating

A linear grating of pitch p with its elements parallel to y-axis is illuminated by a collimated beam and the diffracted waves are collected by the test lens as shown in Fig 13.

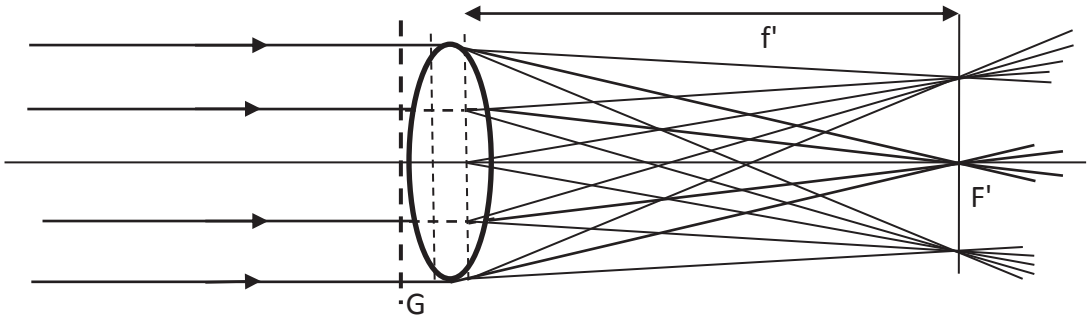

Fig 13. Diffraction at a grating.

Diffraction pattern consisting of bright spots is formed at the back focal plane. The diffraction condition is

$$p \sin\theta_m = m\,\lambda$$

where θ_m is the angle with the optical axis of the m^{th} diffraction order and is expressed as,

$$\sin\theta_m = \frac{y_m}{(y_m^2 + f'^2)^{1/2}} = \frac{y_m}{f'}\frac{1}{(1 + (y_m^2/f'^2))^{1/2}} = \frac{y'_m}{(1 + y'^2_m)^{1/2}}$$

where $y_m/f' = y'_m$ is the normalized coordinate. Hence

$$p \sin\theta_m = \frac{p y'_m}{(1 + y'^2_m)^{1/2}} = m\lambda$$

From this equation, we obtain

$$p^2 y'^2_m = (1 + y'^2_m)\, m^2\lambda^2 \longrightarrow\longrightarrow y'^2_m = \frac{m^2\lambda^2}{(p^2 - m^2\lambda^2)} \rightarrow\rightarrow y'_m = \frac{m\lambda}{(p^2 - m^2\lambda^2)^{1/2}}$$

From this

$$f' = y_m \frac{(p^2 - m^2\lambda^2)^{1/2}}{m\lambda} \cong \frac{y_m p}{m\lambda}\left(1 - \frac{m^2\lambda^2}{2p^2}\right)$$

The focal length is obtained by measuring the locations of the diffraction spots. The uncertainty in the measurement of focal length is obtained from the expression

$$u_f' = \sqrt{\left(\frac{p}{m\lambda} - \frac{m\lambda}{2p}\right)^2 u_{y_m}^2 + \left(\frac{y_m}{m\lambda} - y_m\frac{m\lambda}{2p^2}\right)^2 u_p^2 + \left(\frac{y_m p}{m^2\lambda} + \frac{y_m\lambda}{2p}\right)^2 u_m^2 + \left(\frac{y_m p}{m\lambda^2} + \frac{y_m m}{2p}\right)^2 u_\lambda^2}$$

3.11 Shack-Hartmann Sensor

The Shack-Hartmann sensor consists of a lenslet array and a detector at its focal plane. The lenslet array breaks up the incident wavefront into small sub-apertures. The key assumption is that, over each sub-aperture, the only wavefront variation is local tilt. The tilt is measured by measuring the displacements of the focal spots of each lenslet from their reference positions. This information is used to build the wavefront incident on the lenslet array.

Figure 14 shows a schematic of the experimental se-up that can be used to measure the focal length of a positive lens. The radius of curvature of the wave incident at the Shack-Hartmann sensor is used to measure the effective focal length. The radii of curvature are measured for many locations of the point source P on the optical axis of the test lens and statistical analysis is used to obtain the focal length. Detailed procedure is described in references under Shack-Hartmann Principle.

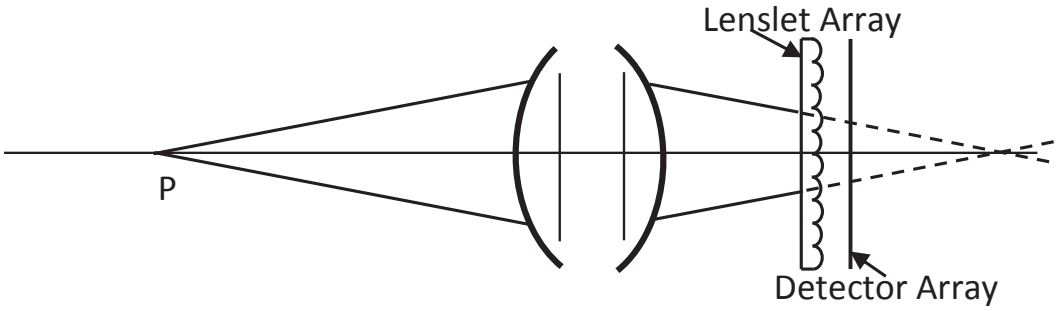

Fig 14. A schematic to measure focal length using a Shack-Hartmann sensor.

3.12 Confocal Method

It is to be noted that most of the methods used for measuring focal length require the detection of back focal plane. There are a number of methods that can be used to locate the plane. One of the methods uses laser speckle phenomenon. As the ground glass surfaces approaches the focal plane, the speckle size keeps on increasing and it becomes very large at the focal plane. In another method, a defocus of 1 wavelength from the true focus results in a dark spot on either side of the focus. These two planes of 1 wavelength defocus can be located, and the true focal plane is midway between them. However, several methods use the confocal arrangement which has strong depth discrimination ability. Methods using this arrangement fall under this category and provide high accuracy of measurement.

3.13 Novel Methods

There are several methods that do not fall under any of the categories described above. For the sake of completion these have been grouped together as references 49 to 70. Readers, if interested, may explore them.

Acknowledgment

Many of these methods are known since long. Some have evolved with the technology. References on this topic have been grouped according to the flow in the tutorial. Hopefully no significant work has been overlooked. Being a tutorial paper, the references are not cited in the text but are provided so that the interested reader may look into the method of interest for details.

References

Collimation Methods

1. Kaul R C, Measurement of focal length through autocollimation method, *J Photo-Int & Remote Sensing*, 9 (1981)17-20.
2. Horner J L, Collimation invariant technique for measuring the focal length of a lens, *Appl Opt*, 28(1989)1047-1048.
3. Ilev I K, Simple fiber-optic autocollimation method for determining the focal lengths of optical elements, *Opt Lett*, 20(1995)527-529.

Talbot Interferometry

4. Nakano Y, Murata K, Talbot interferometry for measuring the focal length of a lens, *Appl Opt*, 24(1985)3162-3166.
5. Bernardo L M, Soares O D D, Evaluation of the focal distance of a lens by Talbot interferometry, *Appl Opt*, 27, (1988)296-301.
6. Chon-Wen Chang, Der-Chin Su, An improved technique of measuring the focal length of a lens, *Opt Commun*, 73(1989)257-262.
7. Der-Chin Su, Chon-Wen Chang, A new technique for measuring the effective focal length of a thick lens or a compound lens, *Opt Commun*, 78(1990)118-122.
8. Bhattacharya J C, Aggarwal A K, Measurement of the focal length of a collimating lens using the Talbot effect and the moiré technique, *Appl Opt*, 30(1991)4479-4480.
9. Sriram K V, Kothiyal M P, Sirohi R S, Talbot interferometry in non-collimated illumination for curvature and focal length measurements, *Appl Opt*, 31(1992)75-79.
10. Sriram K V, Kothiyal M P, Sirohi R S, Direct determination of focal length by using Talbot interferometry, *Appl Opt*, 31(1992)5984-5987.
11. Sriram K V, Kothiyal M P, Sirohi R S, Use of a non-collimated beam for determining the focal length of a lens by Talbot interferometry, *J Opt* (India), 22(1993)61-66.
12. Yang K, Liao Z, Tao T, Analysis of Talbot image symmetry about Fourier spectrum plane and measurement of focal length, *Acta Opt Sin*, 14(1994)50-54.
13. Singh P, Faridi M S, Shakher C, Sirohi R S, Measurement of focal length with phase-shifting Talbot interferometry, *Appl Opt*, 44(2005)1572-1576.
14. Jin X, Zhang J, Bai J, Hou Ch, Hou X, Calibration method for high-accuracy measurement of long focal length with Talbot interferometry, *Appl Opt*, 51(2012)2407-2413.
15. Hao Chen, Yong He, Jianxin Li, Heng Lu, Measurement of long focal lengths with a double-grating interferometer, *Appl Opt*, 52(2013)6696-6702.
16. Luo Jia, Bai Jian, Zhang Jinchun, Hou Changlun, Wang Kaiwei, Hou Xiyun, Long focal-length measurement using divergent beam and two gratings of different periods, *Opt Express*, 22(2014)27921-27931.

Lau Interferometry

17. Thakur M, Shakher C, Evaluation of the focal distance of lenses by white-light Lau phase interferometry, *Appl Opt*, 41(2002)1841-1845.
18. Tay C J, Thakur M, Chen L, Shakher C, Measurement of focal length of lens using phase shifting Lau phase interferometry, *Opt Commun*, 248(2005)339-345.
19. Prakash S, Singh S, Verma A, A low cost technique for automated measurement of focal length using Lau effect combined with Moiré readout, *J Mod Opt*, 53(2006)2033-2042.

Moiré Deflectometry

20. Glatt I, Kafri O, Determination of the focal length of nonparaxial lenses by moiré deflectometry, *Appl Opt*, 26 (1987)2507-2508.
21. Keren E, Kreske M K, Kafri O, Universal method for determining the focal length of optical systems by moiré deflectometry, *Appl Opt*, 27(1988)1383-1385.
22. Trivedi S, Dhanotia J, Prakash S, Measurement of focal length using phase shifted moiré deflectometry, *Opt Lasers Eng*, 51(2013)776-782.
23. Nicola S De, Ferraro P, Finizio A, Pierattini G, Reflective grating interferometer for measuring the focal length of a lens by digital moiré effect, *Opt Commun*, 132(1996)432-436.

24. Angelis M de, Nicola S De, Ferraro P, Finizio A, Pierattini G, Analysis of moiré fringes for measuring the focal length of lenses, *Opt Lasers Eng*, 30(1998)279-286.

Shack-Hartmann Principle

25. Neal D R, Copland R J, Neal D A, Topa D M, Riera P, Measurement of lens focal length using multi-curvature analysis of Shack-Hartmann wavefront data, Proc SPIE, 5523, 243–255, (2004) Current Developments in Lens Design and Optical Engineering V, (14 October 2004); doi.org/10.1117/12.561772.
26. Wu J, Chen J, Xu A, Gao X, Zhuang S, Focal length measurement based on Hartmann-Shack principle, *Optik*, 123(2012)485-488.
27. Senthil Kumar M, Narayanamurthy C S, Kiran Kumar A S, Focal length measurement of microlens array for Shack–Hartmann wavefront sensor using interferometer, *Opt Eng*, 52(2013)124103; doi.org/10.1117/1.OE.52.12.124103 s.
28. Motka L, Measurement of focal length with SHS, *Fine Mech Opt*, 59(2014)43-45.

Interferometry

29. Matsuda K, Barnes T H, Oreb B F , Sheppard C(Jr), Focal-length measurement by multiple-beam shearing interferometry, *Appl Opt*, 38(1999)3542-3548.
30. Kumar Y P, Chatterjee S, Technique for the focal-length measurement of positive lenses using Fizeau interferometry, *Appl Opt*, 48(2009)730-736.
31. Chen L, Hao J, Chen Z, Guo X, Focal length measurement by fiber point diffraction longitudinal interferometry, *Opt Commun*, 322(2014)48-53.
32. Yang Z, Gao Z, Dou J, Wang X, Focal length measurement based on the wavefront difference method by a Fizeau interferometer, *Appl Opt*, 53(2014)5598-5605.
33. Yang G, Miao L, Zhang X, Sun C, Qiao Y, High-accuracy measurement of the focal length and distortion of optical systems based on interferometry, *Appl Opt*, 57(2018)5217-5223.

Confocal

34. Zhao W, Sun R, Qiu L, Sha D, Laser differential confocal ultra-long focal length measurement, *Opt Express*, 17 (2009)20051-20062.
35. Zhao W, Sun R, Qiu L, Sha D, Laser differential confocal radius measurement, *Opt Express*, 18, (2010)2345-2360.
36. Yang J, Qiu L, Zhao W, Wu H, Laser differential reflection-confocal focal-length measurement, *Opt Express*, 20 (2012)26027-26036.
37. Wu H, Yang J, Qiu L, Zhao W, Measuring the lens focal length by laser confocal technique, In Proceedings of the SPIE 8916, (2013)89161E-1-10; doi: 10.1117/12.2035803.
38. Yang J, Qiu L, Zhao W, Li Z, Shao R, Measuring the lens focal length by laser reflection-confocal technology, *Appl Opt*, 52(2013)3812-3817.
39. Zhao W, Li Z, Qiu L, Ren H, Shao R, Large-aperture laser differential confocal ultra-long focal length measurement and its system, *Opt Express*, 23(2015)17379-17393.

Grating Diffraction

40. Sirohi R S, Kumar H, Jain N K, Focal length measurement using diffraction at a grating, in Optical Testing and Metrology III, C P Grover (ed), Proc SPIE 1332,(1990)50-55.
41. Lei F, Dang L K, Measurement of the numerical aperture and f-number of a lens system by using a phase grating, *Appl Opt*, 32(1993)5689-5691.
42. Cao X, Shen S, Chen J, Focal length measurements with a three-grating system, Proc SPIE 1993, 275-282.
43. Lei F, Dang L K, Measuring the focal length of optical systems by grating shearing interferometry, *Appl Opt*, 33 (1994)6603-6608.
44. Nicola S De, Ferrao P, Finizio A, Pierattini G, Reflective grating interferometer for measuring the focal length of a lens by digital moiré effect, *Opt Commun*, 132(1996)432-436.
45. Zhao S, Wen J F, Chung P S, Simple focal-length measurement technique with a circular Dammann grating, *Appl Opt*, 46(2007)44-49.
46. Miks A, Pokorny P, Use of diffraction grating for measuring the focal length and distortion of optical systems. *Appl Opt*, 54(2015)10200-10206.

47. Torcal-Milla F J, Sanchez-Brea L M, Near-field diffraction-based focal length determination technique, *Opt Lasers Eng*, 92(2017)105-109.

48. Yang W, Wang Z, Shen C, Liu Y, Liu S, Li Q, Du W, Song Z, Research on Focal Length Measurement Scheme of Self-Collimating Optical Instrument Based on Double Grating, *Sensors*, 20(2020)2718; doi:10.3390/s20092718

Novel Methods

49. Howland B, Proll A F, Apparatus for the accurate determination of flange focal distance, *Appl Opt*, 11(1970)1247-1251.

50. Nemec J, Measurement of focal length, *Fine Mech Opt*, 16(1971)12-25.

51. Pernick B J, Hyman B, Least-squares technique for determining principal plane location and focal length, *Appl Opt*, 26(1987)2938-2939.

52. Chang C W, Su D C, An improved technique of measuring the focal length of a lens, *Opt Commun*, 73(1989)257-262.

53. Su D C, Chang C W, A new technique for measuring the effective focal length of a thick or a compound lens, *Opt Commun*, 78(1990)118-122.

54. Prakash O, Ram R S, Determination of focal length of convex lenses using Newton's method, *J Opt*, 25(1994)135-138.

55. Angelis M de, Nicola S De, Ferrao P, Finizio A, Pierattini G, A new approach to high accuracy measurement of the focal length of lenses using a digital Fourier transform, *Opt Commun*, 136(1997)370-374.

56. Meshcheryakov V I, Sinelnikov M I, Filippov O K, Measuring the focal lengths of long-focus optical systems, *J Opt Technol*, 66(1999)458-459.

57. Camacho A A, Solano C, Martinez-Ponce G, Baltazar R, Simple method to measure the focal length of lenses, *Opt Eng*, 41(2002)2899-2902.

58. Boo B De, Sasián J, Novel method for precise focal length measurement, in International Optical Design Conference, 2002 OSA Technical Digest Series, (Optical Society of America, 2002), paper IMCS5.

59. Boo B De, Sasián J, Precision focal-length measurement technique with a relative Fresnel-zone hologram, *Appl Opt*, 42(2003)3903-3909.

60. Hou C, Bai J, Hou X, Novel method for testing the long focal length lens of large aperture, *Opt Lasers Eng*, 43 (2005)1107-1117.

61. Bennett H E, Shaffer J J, Test facility for long focal length mirrors, *Proc SPIE*, 1848(2005)117-124.

62. Chollet F, Ashraf M, Simultaneous measurement of focal length and index of refraction of a microlens using a compound microscope, *J Micromech Microeng*, 19(2009)1-8.

63. Malacara-Doblado D, Salas-Peimbertc D P, Trujillo-Schiaffino G, Measuring the effective focal length and the wavefront aberrations of a lens system, *Opt Eng*, 49(2010)053601; doi.org/10.1117/1.3421548.

64. Kim D -H, Shi D, Ilev I K, Alternative method for measuring effective focal length of lenses using the front and back surface reflections from a reference plate, *Appl Opt*, 50(2011)5163-5168.

65. Mafusire C, Forbes A, Mean focal length of an aberrated lens, *J Opt Soc Am A*, 28(2011)1403-1409.

66. Zhu X, Wu F, Cao X, Wu S, Zhang P, Jing H, Focal length measurement of microlens-array by the clarity function of digital image, Proc SPIE, 8417, (2012)84171E.

67. Liao L, Albuquerque BFC de, Parks R E, Sasian J M, Precision focal-length measurement using imaging conjugates, *Opt Eng*, 51(2012)113604; doi.org/10.1117/1.OE.51.11.113604.

68. Dhanotia J, Prakash S, Focal length and radius of curvature measurement using coherent gradient sensing and Fourier fringe analysis, *Optik*, 124 (2013)2115-2120.

69. Pokorný P, Opat J, Mikš A, Novák J, Novák P, Analysis of factors important for measurements of focal length of optical systems. In Proceedings of the SPIE 9628, Optical Systems Design 2015: Optical Fabrication, Testing, and Metrology V, Jena, Germany, 24 September 2015. 96281Z.

70. Ghoorchi-Beygi M, Dashtdar M, Tavassoly M T, Simple digital technique for high-accuracy measurement of focal length based on Fresnel diffraction from a phase wedge, *Meas Sci Technol*, 29(2018)125203.

[*Received*: 08.01.2021; revised recd: 03.02.2021; *accepted*: 01.06.2021]